Cancer Genes and Networks

Molecular Cancer Research

NME1 Drives Expansion of Melanoma Cells with Enhanced Tumor Growth and Metastatic Properties

Ying Wang[1], M. Kathryn Leonard[1], Devin E. Snyder[1], Matthew L. Fisher[1], Richard L. Eckert[1,2], and David M. Kaetzel[1,2]

Abstract

Melanoma is a lethal skin cancer prone to progression and metastasis, and resistant to therapy. Metastasis and therapy resistance of melanoma and other cancers are driven by tumor cell plasticity, largely via acquisition/loss of stem-like characteristics and transitions between epithelial and mesenchymal phenotypes (EMT/MET). NME1 is a metastasis suppressor gene that inhibits metastatic potential when its expression is enforced in melanoma and other cancers. Herein, we have unmasked a novel role for NME1 as a driver of melanoma growth distinct from its canonical function as a metastasis suppressor. NME1 promotes expansion of stem-like melanoma cells that exhibit elevated expression of stem cell markers (e.g., Sox2, Sox10, Oct-4, KLF4, and Ccnb-1), enhanced growth as melanoma spheres in culture, and enhanced tumor growth and lung colonizing activities *in vivo*. In contrast, NME1 expression did not affect the proliferation of melanoma cell lines in monolayer culture conditions. Silencing of NME1 expression resulted in a dramatic reduction in melanoma sphere size, and impaired tumor growth and metastatic activities of melanoma sphere cells when xenografted in immunocompromised mice. Individual cells within melanoma sphere cultures displayed a wide range of NME1 expression across multiple melanoma cell lines. Cell subpopulations with elevated NME1 expression were fast cycling and displayed enhanced expression of stem cell markers.

Implications: Our findings suggest the current model of NME1 as a metastasis-suppressing factor requires refinement, bringing into consideration its heterogeneous expression within melanoma sphere cultures and its novel role in promoting the expansion and tumorigenicity of stem-like cells.

Introduction

Melanoma stem cells (MelSC) have been proposed to drive the growth and progression of melanoma tumors. As with cancer stem cells in general, MelSCs have been posited to be the source of phenotypic heterogeneity within melanoma lesions (1). They exhibit a capacity for self-renewal, but also to initiate and drive tumor growth through their ability to differentiate into proliferative, less tumorigenic melanoma cells. The frequency of MelSCs in melanoma tumors has been associated with malignant progression (2), metastatic potential (3, 4), and poor survival (4) in human melanoma patients.

Metastasis suppressor genes (MSG) have been defined experimentally as genes whose encoded proteins selectively inhibit the metastatic potential of cancer cells, with little or no effect on growth of the primary tumor (5). At least 21 MSGs have been identified to date that selectively inhibit cancer metastasis. The first to be described was NME1 (6), which was initially designated Nm23-h1 (also known as nucleoside diphosphate kinase/NDPK, and Awd in *Drosophila melanogaster*) and was shown to inhibit metastatic activity when overexpressed in cell lines of melanoma and breast cancer origin. Reduced expression of the metastasis suppressor NME1 has been associated with aggressive growth properties in multiple settings of human cancer (7, 8). A variety of molecular mechanisms have been proposed to mediate the metastasis suppressor function of NME1, including its ability to regulate motility-driving signaling pathways (9), transcriptome profiles (10, 11), and genomic stability (12, 13).

Despite the well-recognized link between cancer stem cell phenotypes and metastatic potential in melanoma, the impact of NME1 on the stem-like phenotype of cancer cells had yet to be studied in detail. In the current study, NME1 was shown to be required for growth of melanoma spheres, which are highly enriched for melanoma stem–like cells. We further show NME1 expression promotes expansion of a cell subpopulation within melanoma spheres that exhibit stem-like characteristics (e.g., expression of stem markers Sox2, Sox10, Oct4, Ccnb-1, and CD271). Overall, these studies highlight a novel, unexpected

[1]School of Medicine, University of Maryland-Baltimore, Department of Biochemistry and Molecular Biology, Baltimore, Maryland. [2]Marlene and Stewart Greenebaum Comprehensive Cancer Center, University of Maryland-Baltimore, Baltimore, Maryland.

Note: Supplementary data for this article are available at Molecular Cancer Research Online (http://mcr.aacrjournals.org/).

Y. Wang, M.K. Leonard, and D.E. Snyder contributed equally to the article.

Current address for Matthew L. Fisher: Cold Spring Harbor Laboratory, Cold Spring Harbor, NY 11724.

Corresponding Author: David M. Kaetzel, Department of Biochemistry and Molecular Biology, School of Medicine, University of Maryland-Baltimore, 108 North Greene Street, Baltimore, MD 21201. Phone: 410-706-5080; Fax: 410-706-8297; E-mail: DKaetzel@som.umaryland.edu

Mol Cancer Res 2019;17:1665–74

doi: 10.1158/1541-7786.MCR-18-0019

role played by NME1 in the maintenance of an aggressive cancer stem–like cell phenotype with enhanced tumor growth and metastatic properties.

Materials and Methods

Materials

Unless otherwise specified, reagents were obtained from Sigma-Aldrich (St. Louis).

Cell lines, culture conditions, and melanoma sphere formation assay

The human melanoma cell lines WM9, WM278, WM3211, and 451Lu were gifts of Dr. Meenhard Herlyn (Wistar Institute, Philadelphia, PA). WM9 originated from a metastatic melanoma lesion, while WM278 and WM3211 were derived from vertical phase (VGP) melanomas. 451Lu was originally obtained by selection for enhanced lung metastatic growth after serial xenografting of the metastatic cell line WM164 in immunodeficient mice. WM9, WM278, and 451Lu harbor the $BRAF^{V600E}$ mutation, while WM3211 is BRAF wild-type. Identities of all melanoma cell lines used in this study were verified by short tandem repeat analysis (Biopolymer-Genomics Core Laboratory, School of Medicine, University of Maryland). These lines were maintained and propagated at 37°C in Tu2% medium containing MCDB: Leibovitz-15 medium (4:1 v/v) supplemented with 2% fetal bovine serum (FBS; Life Technologies), 2 mmol/L $CaCl_2$, and 2.5 μg/mL insulin.

Melanoma spheres were generated as described, using a culture medium formulation originally adapted for the propagation and maintenance of neural crest stem cells (14, 15). Monolayer cultures nearing confluence were dissociated into single cells with 0.05% trypsin and suspended in melanoma sphere medium (MM) containing DMEM/F12 (1:1; Gibco), 2% B27 serum-free supplement (Invitrogen), 1% (w/v) methylcellulose, 0.4% (w/v) bovine serum albumin, 20 ng/mL EGF, and 4 μg/mL insulin. Cells were plated at a density of 40,000 cells in individual wells of 6-well dishes (9.6 cm^2/well; Corning), precoated with poly-HEMA to inhibit cell attachment.

Antibodies and immunoblotting

For analysis of impacts of lentiviral shRNA constructs on the expression of relevant proteins, melanoma spheres were harvested 7 days after transduction and lysed in RIPA buffer, consisting of 10 mmol/L Tris-Cl (pH 8.0), 140 mmol/L NaCl, 1 mmol/L EDTA, 1% Triton X-100, 0.1% sodium deoxycholate, 0.1% SDS, and protease inhibitors (Halt Protease Inhibitor Cocktail; Thermo Fisher). Protein concentrations of lysates were measured with the BCA Kit (Thermo Fisher). For immunoblot analysis, SDS-PAGE was conducted using gradient polyacrylamide gels (AnykD Criterion; Bio-Rad). Primary antibodies against the following proteins were used for immunoblotting: Ki67 (sc-15402, Santa Cruz), MITF (sc-56726, Santa Cruz), Ccnb-1 (A305-000A-M, Bethyl Laboratories), CD271 (8238, Cell Signaling Technology), Sox2 (14962, Cell Signaling Technology), Histone-3 (4499, Cell Signaling Technology), NME1 (610247, BD Biosciences), and Oct4 (ab19857, Abcam). The following horseradish peroxidase-conjugated antibodies were obtained from GE Healthcare: sheep anti-mouse IgG (LNA931V/AG) and donkey–anti-rabbit IgG (LNA934V/AG).

Quantitative reverse transcriptase-polymerase chain reaction

Total cellular RNA was isolated from melanoma spheres using the RNeasy Extraction Kit (Qiagen). Purified RNA samples (1 μg) were reverse transcribed using the High Capacity cDNA Reverse Transcription Kit (Applied Biosystems). Quantitative real-time PCR (qRT-PCR) was conducted on a Bio-Rad CFX Connect Real-Time PCR Detection System using the Power SYBR Green PCR kit and primers specific for RNA transcripts of interest. PCR was conducted with an initial 3-minute incubation at 95°C, followed by 40 cycles of 95°C for 30 seconds and 62.5°C for 30 seconds. Relative RNA expression was calculated using the $2^{-\Delta\Delta CT}$ method, and expressed relative to that of a reference gene (RPL13). The following forward PCR primers were used: NME1, 5′-ccggtccg-ccttgttggtctgaaatct-cgagatttcagaccaacaaggcggattttt-3′; NME2, 5′-ctctctgctctcccagcgcag-3′; ALDH1a (sense), 5′-ctgctggcgacaatg-gagt-3′; CD271, 5′-acctccagaacaagacctcatagc-3′; CD133, 5′-cctggggctgctgtttatta-3′; Sox2, 5′-cagctcgcagacctacatga-3′; Sox10, 5′-tttgactactctgaccatcagccc-3′; Ki67, 5′-gaggtgtgcagaaaatccaaa-3′; Ccnb1, 5′-cgatcgccctggaaacgcattc-3′; MITF-M, 5′-ttatagtaccttctc-tttgccagtcc-3′; RPL13, 5′-cataggaagctgggagcaag-3′. The following reverse primers were used: NME1, 5′-aattaaaaatccgccttgttggtct-gaaatctcgagatttcagaccaacaaggcgga-3′; NME2; 5′-gtccggcttgatggc-gatgaag-3′; ALDH1a, 5′-gtcagcccaacctgcacag-3′; CD271, 5′-ttgttctgcttgcagctgttcc-3′; CD133, 5′-ttgatccgggttcttacctg-3′; Sox2, 5′-tggagtgggaggaagaggta-3′; Sox10, 5′-agtgtcgtatatactggctgctcc-3′; Ki67, 5′-ctgtccctatgacttctggttgt-3′; Ccnb1, 5′-ccagcagaaaccaacag-ccgttc-3′; MITF-M, 5′-gtttatttgctaaagtggtagaaaggtact-3′; RPL13, 5′-gccctccaatcagtcttctg-3′.

Lentiviral constructs and melanoma sphere transduction

The 293T host cell line was used for lentivirus production and was propagated in DMEM supplemented with 10% FBS and 1 mmol/L sodium pyruvate. Production of lentiviral shRNA expression vectors was initiated by cotransfection of 293T cells (2.5×10^6/10 cm dish) with three plasmid vectors: pLENTI-17531 (4 μg) and pCMV-VSVG (0.67 μg), both provided by the Virus Core Facility, University of Maryland School of Medicine, and a plasmid (pLKO.1-puro, 4 μg; Sigma Mission shRNA) harboring one of three shNME1 sequences. The three plasmids and Fugene 6 Transfection Reagent (Promega) was mixed with 600 μL DMEM and incubated with cells for 12 hours, followed by replacement with fresh complete media. Transfected cells were maintained in culture for 3 days, followed by three successive 12-hour periods of virus collection. Conditioned medium containing viral particles was pooled, filtered (0.45 mmol/L), and stored in aliquots at −80°C prior to use. shNME sequences were as follows: shNME1a, 5′-ctagttatttacaggaactt-3′; shNME1b, 5′-tccgccttgttggtctgaaat-3′; shNME1c, 5′-gcgtaccttcattgcgatca-3′. Melanoma spheres were dissociated into single cells by trypsinization prior to viral transduction. Cells were transduced with a mixture of lentivirus-containing supernatants and polybrene (8 μg/mL in DMEM). Cells were then resuspended in MM and transferred to 48- or 6-well dishes with nonadherent HEMA-coated surfaces for melanoma sphere formation.

Flow cytometry analysis and fluorescence-activated cell sorting

Flow cytometric analysis of melanoma sphere cells. For membrane staining with the dye PKH26 and monitoring for label retention, melanoma spheres were dissociated into single-cell suspensions with trypsin and incubated with the dye as per the manufacturer's instructions (PKH26 Red Fluorescent Cell Linker Kit, Sigma).

Stained cells were used for melanoma sphere formation assay as described above, at a density of 120,000 cells/well in 10 cm nonadherent dishes. After 3 weeks of growth, melanoma spheres were dissociated into single cells with trypsin and analyzed for PKH26 retention and expression of relevant proteins by flow cytometry. For immunostaining, cells were fixed with 2% formaldehyde, and subjected to membrane permeabilization with 0.7% (v/v) Tween-20 in phosphate-buffered saline (PBS). Primary and secondary antibodies were diluted in staining buffer [PBS, 10% (v/v) goat serum, 1% (w/v) bovine serum albumin, 0.5% Tween-20] and incubated with cells for 30 minutes at room temperature. Antibody-containing solutions were removed, followed by two washes and resuspension in PBS prior to flow cytometry. The following primary antibodies were obtained from BD Biosciences: V450-conjugated mouse anti-Sox2 (561610), PerCP-Cy5.5-conjugated anti-Oct-4 (560794), PECy7-conjugated anti-Ki67 (561283), and mouse monoclonal anti-NME1 (610247). Secondary antibodies used were: FITC Rat anti-mouse IgG (406001, BioLegend) and Apc-Cy7 donkey anti-goat IgG (H2615, Santa Cruz).

Flow cytometric analysis of melanoma cells from xenografts in NSG mice. Single-cell suspensions were generated from mouse lungs harboring GFP-expressing melanoma cells (experimental metastasis) by incubation of lung pairs in 5 mL of dissociation solution (PBS containing 0.25% trypsin, 2.2 mmol/L EDTA; PBS-TE) at 37°C for 15 minutes. Trypsin activity was quenched by addition of 0.5 mL of 100% FBS followed by rigorous pipetting. After a brief period (1–2 minutes), supernatants were collected, centrifuged ($400 \times g$, 5 minutes), and resuspended in 3 mL of FBS. Undigested tissue fragments were rinsed with PBS and subjected to 3 to 4 additional cycles of trypsin treatment, with pelleted cells from all cycles pooled into the same 3 mL of FBS. Pooled cells were centrifuged, resuspended in PBS, and single cells isolated for flow cytometry by filtration through a 70-μm cell strainer. Dead cells were detected by staining with the Fixable Violet Dead Cell Stain Kit (Thermo Fisher). Primary antibodies differing from those described previously were PE-conjugated rabbit monoclonal anti-Axl (78909S, Cell Signaling Technology), mouse monoclonal anti-MITF-M (sc-56726, Santa Cruz), rabbit polyclonal anti-Oct-4 (ab19857, Abcam), goat polyclonal anti-Sox2 (sc17320, Santa Cruz), and rabbit polyclonal anti-Ki67 (sc15402, Santa Cruz). Secondary antibodies used were PE Rat anti-Mouse IgG (562021, BD), PE donkey anti-Rabbit IgG (406421, BioLegend), and Alexa Fluor 488 donkey anti-rabbit IgG (A21206, Life Technologies).

Xenografting of melanoma cells in NSG mice

Mouse care, surgery, and injection protocols were approved by the Institutional Animal Care and Use Committee at the University of Maryland-Baltimore (protocol number 0515008). Melanoma spheroid cells were prepared for xenografting experiments by introducing expression of enhanced GFP (eGFP) using a lentiviral expression vector (lentiviral plasmid pSMPUW-MCV-ccd-eGFP). Transduced cells were seeded in 10-cm dishes and expanded under monolayer conditions. Single-cell suspensions were prepared by trypsinization, followed by sorting of eGFP-positive cells by FACS. eGFP-positive cells were cultured as melanoma spheres in MM for 7 days, followed by transduction with lentiviral vectors expressing shRNAs of interest, and growth as melanoma spheres for 4 days. Cells were prepared from spheres for injection by dissociation with trypsin, pelleting, and resuspension in a solution of 30% Matrigel in PBS (Corning).

Primary tumor growth and experimental metastasis in NSG mice. For the generation of primary tumor xenografts, 10^5 cells (100 μL volume) were injected subcutaneously into the rear flank of 7- to 8-week-old NSG (NOD.Cg-*Prkdc*^{scid} *Il2rg*^{tm1Wjl}/SzJ) mice. Measurements of tumor dimensions were obtained twice per week. Tumor volume was calculated as $V = L \times W \times H \times \pi/6$ (V, tumor volume; L, length; H, height).

For experimental metastasis, 451Lu cells were transduced for eGFP expression and used to generate melanoma spheres, followed by the preparation of single-cell suspensions for injection, as described above. Cells (10^5 cells/100 μL) were injected into the lateral tail vein of 7- to 8-week-old NSG mice. Mice were euthanized at 38 to 40 days after injection, lungs were removed, rinsed in PBS, and assessed for the presence of eGFP-labeled colonies using a Leica M210F UV dissection microscope. Numbers and sizes of melanoma colonies were quantified using the "Grid" and "Cell Counter" plug-ins of the imaging platform ImageJ.

Results

NME1 expression drives proliferation of stem-like cells in melanoma sphere culture

Tumor cells often form sphere structures (tumor spheres) when cultured on nonadherent surfaces in media optimized for the growth of stem-like cells. Tumor sphere–derived cells exhibit elevated abilities to drive initiation, maintenance, and progression of malignant lesions in a number of settings of human cancer (16), including melanoma (2–4). Melanoma spheres grown in media optimized for neural crest cells are heterogeneous (17), but enriched for cells that express proteins associated with stemness (18). To measure the impact of the metastasis suppressor NME1 on the growth of melanoma spheres, NME1 expression was silenced using multiple shRNAs directed to the NME1 transcript. The analysis was conducted with two metastatic lines, 451Lu and WM278, and the vertical growth phase (VGP) melanoma-derived cell line WM3211. All three lines formed robust melanoma spheres when grown under sphere-promoting conditions (Fig. 1A and B). In contrast, suppression of the NME1 transcript with shRNA (shNME1a; Fig. 1B) dramatically reduced the formation and growth of melanoma spheres in all three cell lines. The shNME1a sequence effectively silenced NME1expression and had no off-target effects on the related NME2 isoform in any of these three cell lines, with the exception of a small decrease in NME2 RNA in WM3211 cells (Fig. 1C; Supplementary Fig. S1). The inhibitory effect of shNME1a on sphere formation was reproduced in WM278 and WM3211 with two additional shRNA sequences (shNME1b and shNME1c; Fig. 1B, middle), and in 451Lu cells with the shNME1a and shNME1b constructs (Fig. 1B, right). The shNME1b and shNME1c sequences also selectively inhibited the NME1 transcript with minimal effects on NME2 expression (Supplementary Fig. S1). Conversely, forced expression of NME1 strongly promoted growth of melanoma spheres in three different cell lines, WM3211, WM278, and M14 (Fig. 1D). Silencing of NME1 expression had no impact on the growth of WM9, WM278, or 451Lu cell lines in monolayer culture conditions (Fig. 1E).

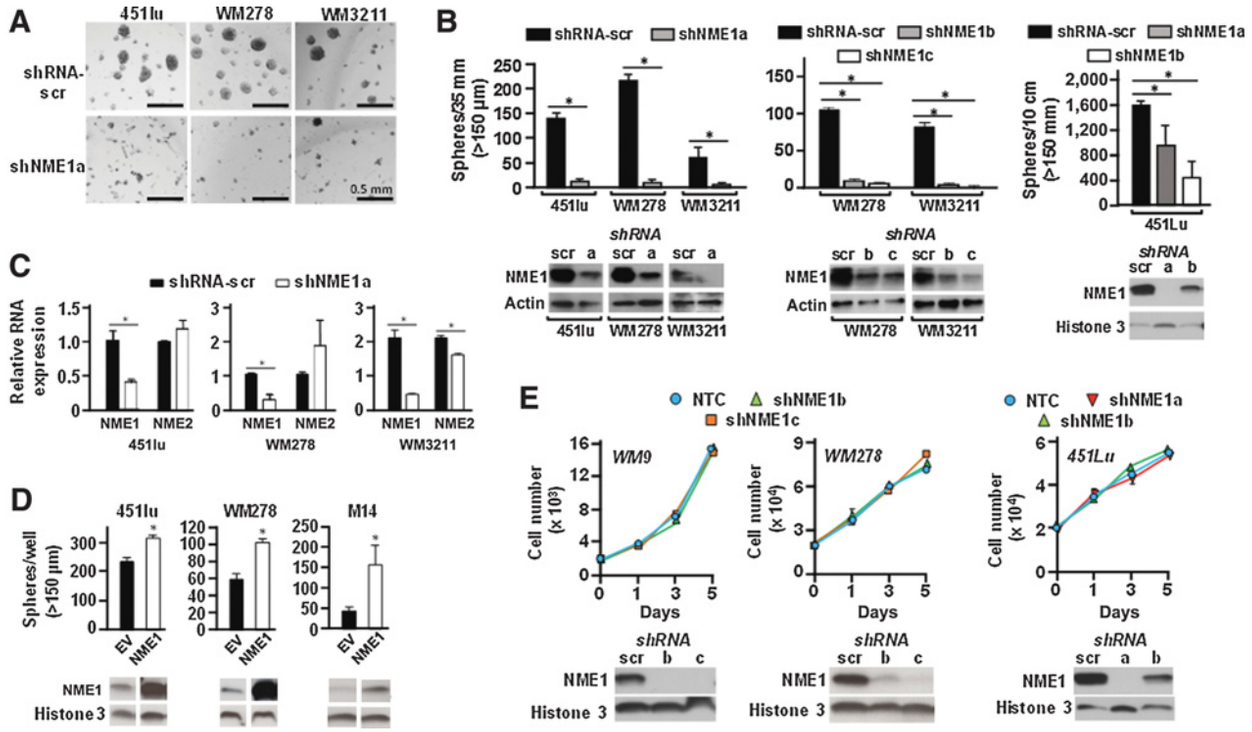

Figure 1.

NME1 selectively promotes the growth of melanoma spheres without impact on cell proliferation in monolayer culture conditions. Cells of the three indicated melanoma lines (451Lu, WM278, and WM3211) were infected for 24 hours with lentiviruses expressing either a scrambled shRNA sequence (shRNA-scr) or one of three shRNAs targeting NME1 (shNME1a-c). Cells were then seeded as indicated in the figure in individual wells of 6-well dishes (4×10^4 cells/well) or 10-cm dishes (3×10^5 cells/plate) containing an ultralow attachment surface, and grown in spheroid medium for varying lengths of time. **A,** Shown is melanoma sphere formation obtained after 7 days of growth following infection with shRNA-scr or shNME1a. **B,** The left subpanel displays quantification of melanoma spheres from the study of **A**. The middle subpanel displays melanoma sphere incidence after infection with one of two additional shNME1 constructs (shNME1b and shNME1c) and a 16-day period of growth. The right subpanel summarizes the effect of shNME1a and shNME1b in 451Lu cells. Efficacy of shNME1-mediated silencing was verified by immunoblot analysis, as shown below the graphs in each subpanel. shNME1c did not provide robust silencing of NME1 expression in 451Lu cells (not shown). **C,** Efficacy of NME1 knockdown was assessed in terms of NME1 RNA expression by quantitative reverse transcriptase real-time polymerase chain reaction (qRT-PCR). NME1 RNA is expressed relative to that observed in cells infected with the shRNA-scr control lentivirus ("Relative RNA expression"). Expression of the NME2 transcript was also measured by qRT-PCR to verify specificity of the respective shNME1 constructs. **D,** Forced expression of NME1 promotes melanoma sphere growth. Cells were infected as shown with lentiviruses expressing the indicated shRNA constructs in combination with empty lentivirus (EV) or a virus expressing NME1. M14c3 is a clone selected for high levels of forced NME1 expression. **E,** shNME1-mediated silencing does not affect proliferation of melanoma cell lines in monolayer culture. Cells of the indicated melanoma-derived lines were seeded in 24-well dishes (2×10^4 cells/well), with cells counted manually at the indicated time points. All data in the figure are derived from 2 to 3 independent experiments. For all panels: *, $P \leq 0.05$.

Immunoblot analysis was used to assess the effect of silencing NME1 expression on expression of proteins indicative of proliferative index, stemness, and differentiation in melanoma cell lines under both monolayer and sphere culture conditions (Fig. 2). Silencing of NME1 with the shNME1a sequence in monolayer cultures of 451 cells had no effect on expression of three stem cell marker proteins (Oct4, Jarid1b, and CCNB1), with perhaps a small inhibitory effect on the stem marker KLF4 (Fig. 2A, left). In the setting of sphere culture conditions for 451Lu cells, expression of all four stem cell markers was higher than in monolayer conditions, consistent with enrichment of stem-like cells (Fig. 2A, right). In contrast with the monolayer condition, NME1 silencing in 451Lu sphere conditions strongly inhibited expression of all four stem markers. Expression of the proliferation marker Ki67 was inhibited by NME1 silencing to a minimal extent in monolayer growth conditions, and not at all in sphere conditions. This indicates the shNME1a treatment did not inhibit cell proliferation of the bulk population *per se*, but rather the ability of cells to grow as melanoma spheres. Interestingly, NME1 silencing in WM278 monolayers inhibited expression in three of the four stem cell marker proteins (Jarid1b, CCNB1, and Sox2), although not that of Oct4 (Fig. 2B, left). Thus, the WM278 cell line retains considerable stem-like character under monolayer conditions, and the stem-like phenotype in both monolayer and sphere growth conditions is NME1 dependent. Consistent with this observation, a slow-cycling subpopulation with elevated JARID1B expression has been observed in human melanoma cell lines under monolayer culture conditions (17). NME1 silencing had no effect on Ki67 expression in WM278 monolayers and was only modestly inhibitory in WM278 spheres, again demonstrating that NME1 had little effect on the proliferation of the bulk compartment under either culture condition.

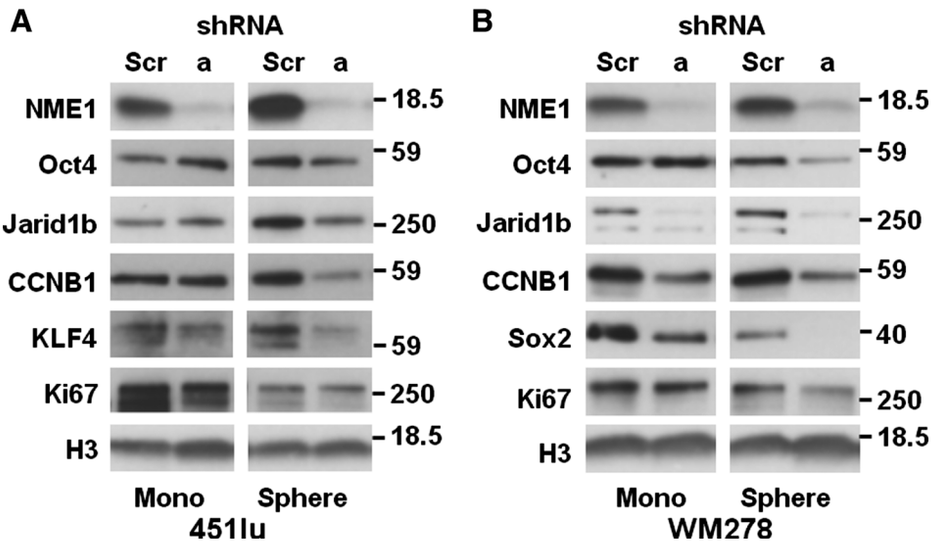

Figure 2.
NME1 regulates expression of proliferation and stem cell markers. Immunoblot analysis was used to measure expression of stem cell and proliferation markers in monolayer ("Mono") and sphere cultures after shRNA-mediated silencing of NME1 in (**A**) 451Lu or (**B**) WM278 cells.

Fast-cycling melanoma sphere cells express elevated levels of NME1 and exhibit stem-like characteristics

Melanoma spheres contain cell subpopulations that are heterogeneous with respect to indices of proliferation, stemness, and melanocytic differentiation (17). Having demonstrated that silencing of NME1 expression perturbed the proliferative and stem-like characteristics of melanoma sphere cultures, we explored the extent to which endogenous NME1 expression was associated with these phenotypes in individual sphere cells. Slow- and fast-cycling cells were distinguished by labeling of cells with the membrane-staining dye PKH26 prior to generation of melanoma spheres. PKH26-labeled WM9 and WM278 cells were grown as spheres for 3 weeks, dissociated into single-cell suspensions, stained for intracellular NME1, and subjected to FACS analysis. Small subfractions (0.05%–0.5%) of PKH26-retaining cells (i.e., slow-cycling) were observed in melanoma spheres derived from both cell lines (Fig. 3A). Interestingly, NME1 expression was heterogeneous and wide-ranging across the cell populations. Sphere cells from the two cell lines were sorted into six distinct subpopulations, based on the intensity of staining of PKH26 and level of NME1 expression. One small subpopulation of slow-cycling cells exhibited low expression of NME1 (Fig. 3A, top left box of both plots), while another expressed higher levels of NME1 (top right). NME1 expression was also elevated in subpopulations that had undergone modest (middle right box) or total (bottom right) loss of the PKH26 dye. Another subpopulation represented cells that had lost PKH26 staining and expressed NME1 at low levels (bottom left).

To identify potential correlations between NME1 expression and cell phenotypes within melanoma sphere cultures, the six subpopulations were isolated by FACS and individually analyzed by flow cytometry for expression of Ki67 and the stem cell markers SOX2, SOX10, and OCT4. Cells from WM9-derived melanoma spheres exhibited a consistent correlation in expression of NME1 and Ki67, regardless of the level of PKH26 retention (Fig. 3B). Of additional note was the coordinately high expression of Ki67 and NME1 in a small subpopulation of WM9 cells that had not lost PKH26 staining (top right square, Fig. 3A), suggesting those cells had initiated but not completed a mitotic event. The two other subpopulations in which NME1 expression was elevated (middle and bottom right, Fig. 3A) also exhibited elevated Ki67 expression relative to their low NME1 counterparts. Together, these observations indicated that elevated NME1 expression was associated with cells that were either fast-cycling or undergoing their first mitosis, strongly suggesting that NME1 expression was required for their proliferation. Similar strong correlations were seen in WM9-derived spheres across the subpopulations between expression of NME1 and the stem markers SOX2, SOX10, and OCT4 (Fig. 3B). The subpopulation of cells that lost PKH26 staining and expressed low levels of NME1 (bottom left) may have acquired a differentiated phenotype or reacquired the slow-cycling stem-like phenotype of the top left subpopulation. Nearly identical results were obtained in a similar analysis of WM278-derived spheres, although more cells were observed in the high-NME1, slow-cycling subpopulation than in WM9 spheres (Fig. 3A and C). This difference could be attributed to phenotypic differences between cell lines derived from similar, but distinct melanoma lesions with different oncogenic machinery at play. Similar to the WM9 cell line, however, Ki67 expression was significantly elevated in this subpopulation, suggesting these cells were also poised for mitosis. Cumulatively, the analysis of proliferation and stem markers strongly suggests that NME1 drives expansion of a stem-like subpopulation in melanoma sphere cultures.

NME1 expression promotes tumor growth and lung colonization (experimental metastasis) potential of melanoma sphere cells

To assess the impact of NME1 expression on the malignant properties of cells derived from melanoma sphere culture, xenografting studies were conducted in NSG mice. Melanoma sphere cultures were generated from the WM278 and 451Lu cell lines following transduction with lentiviruses driving expression of scrambled or NME1-directed shRNA sequences, as well as the fluorescence marker eGFP. Prior to injection, melanoma sphere cultures were dissociated, sorted for eGFP expression by FACS, and viability of sorted cells verified by trypan blue staining. WM278-derived melanoma spheres infected with the scrambled shRNA grew rapidly as subcutaneous xenografts, achieving critical size within 52 days after injection (Fig. 4A and B). Transduction with the shNME1a sequence, however, almost completely

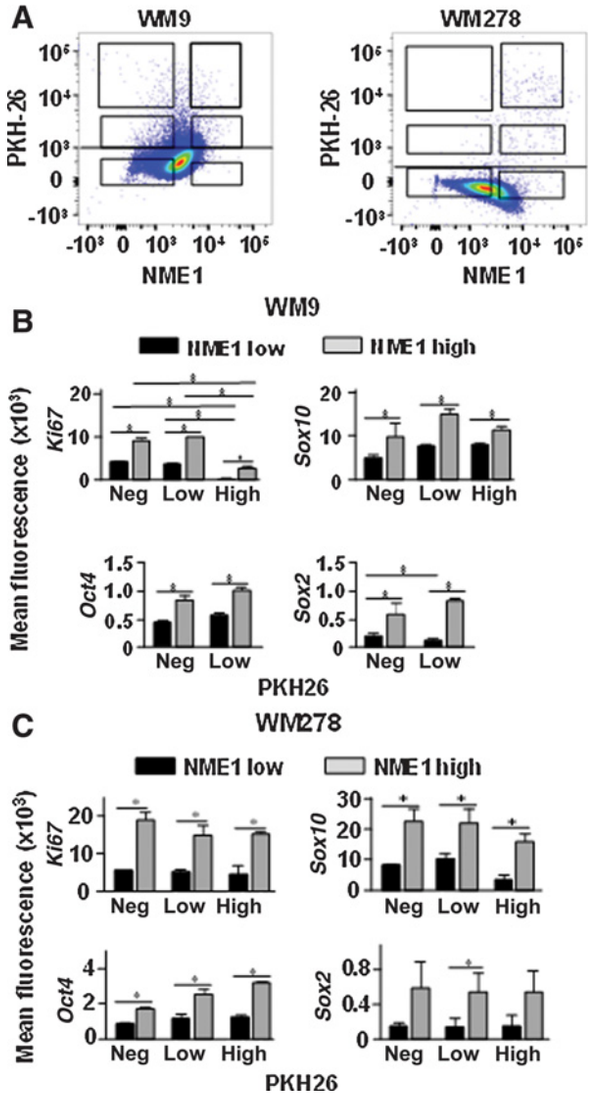

Figure 3.

Melanoma sphere cultures contain subpopulations of proliferative cells that exhibit increased expression of NME1 and stem cell markers. Melanoma spheres were grown for 21 days after labeling with PKH26 and analyzed by flow cytometry after staining with antibodies specific for NME1, stem cell markers (Sox2, Sox10, Oct4), and Ki67. **A,** Dot plot gatings based on levels of NME1 and PKH26 dye retention in WM9 (left) and WM278 (right) sphere cells. **B** and **C,** Mean fluorescence of stem cell markers and Ki67 staining for the gated populations from sphere cells of **A**. **B,** WM9; **C,** WM278. Means ± SEM derived from cumulative data of three independent experiments are shown; *, $P < 0.05$.

abrogated the growth of sphere-derived cells as tumor xenografts (Fig. 4A and B). NME1 depletion also inhibited the growth of tumors initiated with cells from 451Lu melanoma spheres (Fig. 4A and B).

To quantify the impact of NME1 depletion on tumor-initiating activity, an extreme limiting dilution assay (ELDA) was conducted with subcutaneous injections of 1000, 100, and 10 cells from WM451-derived melanoma sphere cultures, prepared as described above. Overall average tumor size at the 52-day endpoint was significantly larger in the scrambled shRNA group at both 100 and 10 cells/injection (Fig. 4C). No significant difference in tumor incidence was observed between the control and shNME1-treated groups at the 100 cells/injection condition, but a lower incidence was detected at 10 cells/injection (Fig. 4D). ELDA revealed a significant shNME1-mediated decrease ($P < 0.03$) in the incidence of detectable xenograft tumors at 45 days after injection (Fig. 4E). This effect was not maintained through the 52-day time point, suggesting the eventual acquisition of alternative stemness-driving mechanism(s) that circumvented the shNME1 treatment. Nevertheless, these studies collectively indicate that NME1 depletion strongly impairs the growth and stem-like character of melanoma cells grown in sphere culture conditions, and significantly impairs their ability to initiate tumors *in vivo*.

We also assessed the impact of NME1 on the ability of melanoma sphere cells to colonize lung tissues when injected via the tail vein (experimental metastasis). Injection of eGFP-labeled melanoma sphere cells transduced with scrambled shRNA (10^5 cells/injection) elicited numerous and robustly growing colonies in both lungs of all mice within 38 days of injection (Fig. 5A and B). Transduction with the shNME1a sequence resulted in a dramatic reduction in lung colonization potential of melanoma sphere cells, with 60- to 100-fold higher colonies/lung and greatly increased size per colony in scrambled shRNA-expressing cells (Fig. 5A and C). Strong reductions in lung colonizing activity were also observed with the shNME1b sequence (Fig. 5B and D).

Discussion

Silencing of NME1 expression strongly impaired the sphere-forming activity of melanoma cells (Fig. 1) and loss of a fast-cycling subpopulation of cells with stem-like characteristics. In addition, cells derived from NME1-depleted melanoma spheres exhibited reduced tumor growth as orthotopic xenografts within the skin, or when seeded in the lung via the tail vein. ELDA analysis revealed a significant delay in tumor initiation for NME1-depleted cells. The inhibitory effect did not persist indefinitely, however, suggesting the eventual co-option of alternative stem-inducing pathways. We further observed that NME1 expression is heterogeneous within melanoma spheres and, consistent with the NME1 depletion analyses, elevated NME1 expression is associated with the fast-cycling/stem-like subpopulation. Taken together, our observations indicate that NME1 drives the proliferation of sphere cells with enhanced ability to grow as primary tumors and colonize lung tissues.

The enhanced tumor growth properties of NME1-expressing cells in sphere culture might initially appear to be incongruent with the long-recognized classification of NME1 as an MSG, a gene that suppresses metastatic potential of tumor cells without impact on their growth in cell culture or as tumors *in vivo*. We would note that our study differed significantly from prior reports by the extensive use of shRNA-mediated gene silencing. Gene silencing technologies have been applied sparingly to studies of NME1 function, particularly in comparison with the extensive number of reports using forced/constitutive NME1 expression (19). Most studies using NME1 silencing have focused on phenotypes of motility and invasion *in vitro*, and used cells maintained in standard monolayer/serum-stimulated culture conditions. Moreover, to our knowledge, no prior studies have evaluated the impact of NME1 silencing on metastatic phenotypes

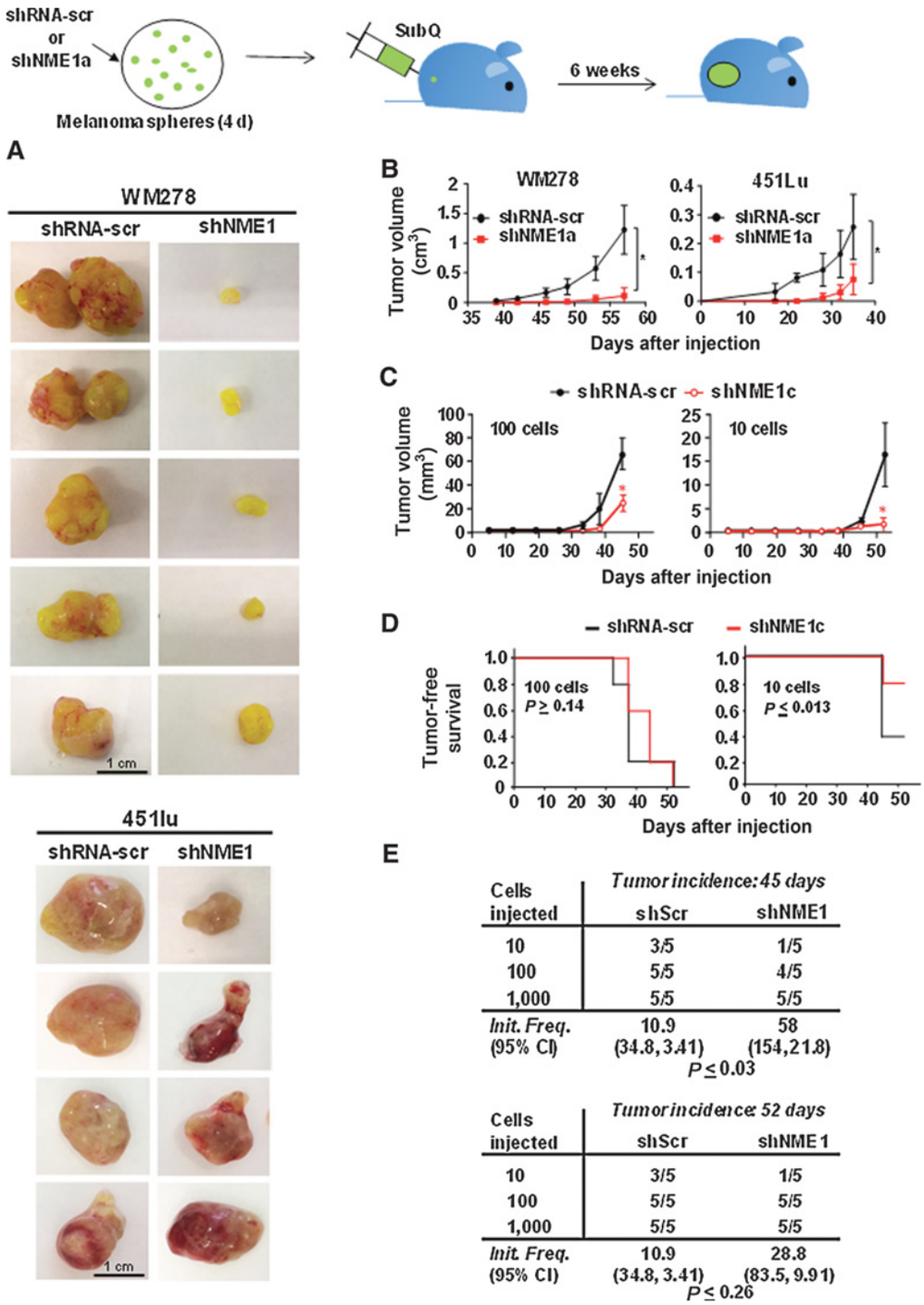

Figure 4.

NME1 promotes tumor growth properties of cells derived from melanoma sphere cultures. Melanoma sphere cells from WM278 or 451lu cell lines were cultured and transduced with lentivirus expressing either shRNA-scr or shNME-1a. Four days after viral transduction and growth in sphere culture, cells were dissociated into single cells and injected subcutaneously into the rear flank of NSG mice. **A,** Tumor xenografts from WM278- and 451Lu-derived cells at the experiment endpoint (5.5 weeks or tumor size > 1 cm^3). **B,** Tumor growth curves obtained after subcutaneous xenografting of sphere cells derived from the WM278 (left) and 451Lu (right) cell lines in NSG mice. Data points represent mean ± SEM ($n = 5$, $P \leq 0.05$). Growth curves were compared using a regression ANOVA model. **C,** Growth of 451Lu xenografts initiated with either 100 or 10 cells. Asterisks denote means that are significantly different ($P \leq 0.05$). **D,** Kaplan–Meier plots of tumor-free survival after subcutaneous injection of 451Lu sphere cells (100 or 10, $n = 5$). Differences in tumor-free survival between the treatment groups were determined using the log-rank test. **E,** After 52 days, mice were euthanized and tumor-initiating frequency was calculated using extreme limiting dilution analysis (ELDA), as described (28).

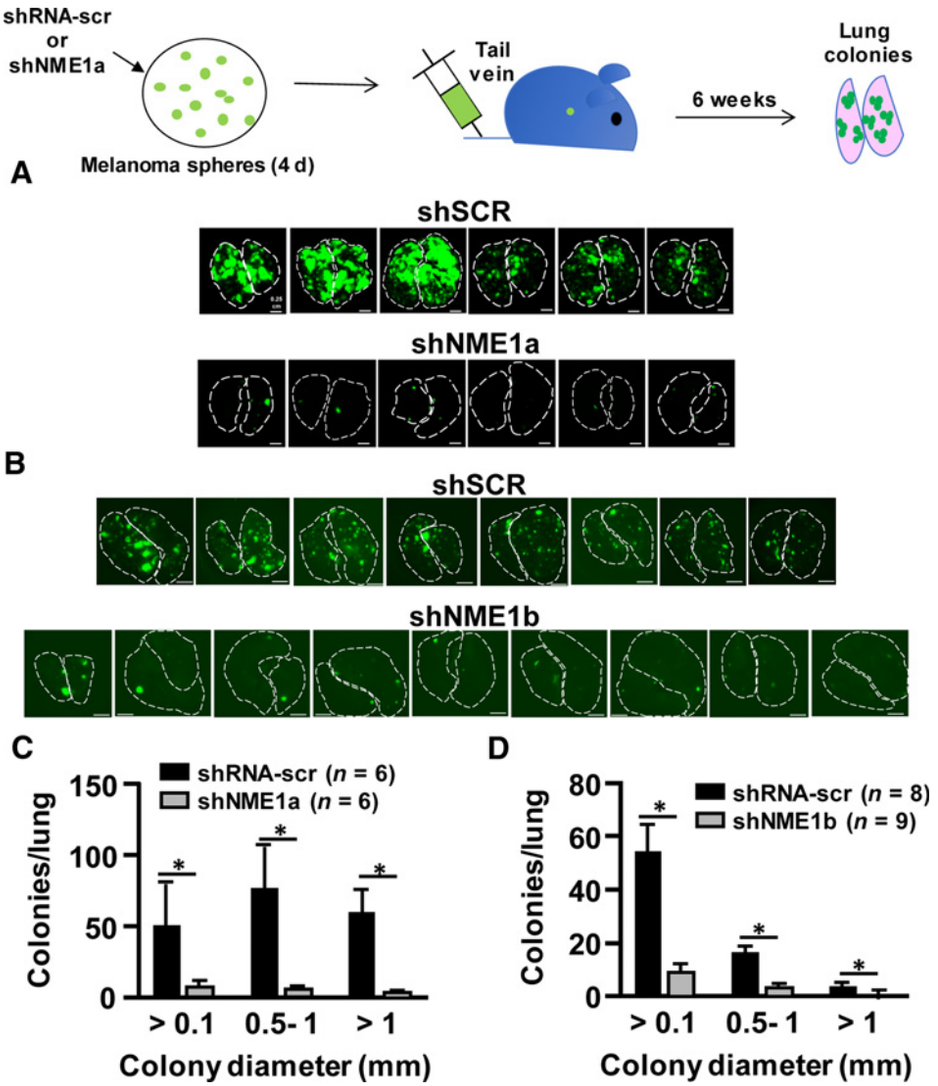

Figure 5.
NME1 promotes colonization of melanoma sphere–derived stem cells in lung tissue (experimental metastasis). 451Lu cells expressing eGFP were treated with lentiviruses expressing shRNA-scr, shNME1a, or shNME1b as indicated, and used to generate melanoma spheres. After 4 days of melanoma sphere growth, cultures were dissociated into single cells and injected into the tail veins of NSG mice (10^5 cells/mouse). Lungs were imaged for eGFP fluorescence at 5.5 weeks after injection. **A,** eGFP-expressing lung colonies from 451Lu cells expressing shRNA-scr or shNME1a. Outlines of left and right lungs are denoted with dotted lines. **B,** Lung colony formation from 451Lu cells expressing shRNA-scr or shNME1b. **C,** Quantification of colony formation in lungs shown in **A**. *, $P \leq 0.02$. **D,** Quantification of colony formation in lungs shown in **B**.

in vivo. In addition, we compared the impact of NME1 under conditions for cell growth as monolayers and melanoma spheres. Sphere culture conditions unmasked a unique ability of NME1 to stimulate growth properties of melanoma cells, an effect not seen when propagated under monolayer conditions (20, 21). Dependence on NME1 for tumor growth-competence of cells grown in sphere culture could be attributed to the nonadherent growth conditions, cell contact–driven signaling in spheres, the medium itself (B27 supplement, EGF, insulin, etc.), or combinations thereof. Alternatively, standard monolayer culture conditions (e.g., cell adhesion to plastic, FBS) could inhibit the effects of NME1 expression seen in sphere culture.

The observation that both monolayers and melanoma spheres retain a small, slow-cycling cell subpopulation with lower expression of NME1 and stem markers than the faster-cycling bulk population strongly suggests that NME1 expression is dynamic both *in vitro* and *in vivo*. In light of the apparent impact of NME1 expression on cell phenotypes in sphere culture, dynamic regulation of NME1 expression may regulate phenotypic transitions in cancer cells as well. Such a model could explain the paradox of how NME1 appears to function as a canonical metastasis suppressor gene in some experimental settings, yet drives expansion of cells in sphere culture with increased tumor growth properties. Almost all studies presented in support of a metastasis suppressor function for NME1 have used forced NME1 expression in the context of monolayer culture conditions. In this scenario, NME1 expression may have no effect on proliferation of the bulk cell compartment in which endogenous NME1 expression is sufficient to maintain proliferation, particularly in monolayer cultures. However, overriding dynamic regulation of endogenous NME1 by forced expression could interfere with phenotypic transitions (e.g., ability to transiently downregulate NME1) needed to negotiate the multiple barriers to metastasis. The end result of forced NME1 expression in this scenario would indeed be reduced metastatic activity. Conversely, chronic shNME1 treatment could interfere with transient upregulation of endogenous NME1 expression required for other phenotypic transitions that also drive tumor expansion and metastasis. Assessing the extent to which fast-cycling cells driven by NME1 are fully self-renewing or undergoing differentiation via a transit-amplifying

phenotype (22) may prove informative in this regard. NME1 expression has indeed been associated with differentiation in the setting of nontransformed cells (23–25). It should also be recognized that the tumor microenvironment is likely to regulate the interplay between NME1 expression and tumor cell phenotype. Although further examination of these scenarios will require new experimental approaches for assessing the impact of NME1 on cell fates, our studies demonstrate that the description of NME1 solely as a suppressive entity in cancer appears to require refinement.

The observation that cells derived from melanoma sphere culture are heterogeneous with respect to NME1 expression is intriguing, in light of our demonstration that NME1 promotes genomic stability. NME1 expression is associated with higher efficiency of repair of ultraviolet light-induced lesions in DNA (13, 26). We have more recently observed that NME1 is recruited directly to double-strand DNA breaks, where it promotes the nonhomologous end-joining pathway (NHEJ) of double-strand break repair (Puts and colleagues, submitted). Considering the error-prone nature of NHEJ, these findings suggest the fast-cycling, high NME1 condition accelerates acquisition of progression-driving mutations. Studies are ongoing to analyze the impact of NME1 expression on the genomic stability of the various subpopulations of cells we have identified within melanoma sphere cultures.

Although reduced expression of NME1 has been associated with increased metastasis and shorter survival across a spectrum of human cancers (27), it has not proven a robust prognostic or diagnostic marker for the management of cancer patients. Our observation of heterogeneous expression of NME1 within melanoma sphere cultures suggests that similar heterogeneity exists within melanoma tumors *in vivo*, which could complicate the interpretation of NME1 protein or RNA expression in histopathologic analyses. Our studies pose the intriguing possibility that relative numbers of cells with low and high NME1 expression in tumor specimens, rather than the average intratumoral expression of NME1 transcripts or protein, could be more closely associated with poor prognosis in melanoma.

Our study has identified a novel role for NME1 in the context of melanoma sphere cultures, where it promotes expansion of cells with enhanced tumor and metastatic potential. Further study must be focused on the extent to which NME1 expression is indeed heterogeneous in melanoma specimens, and the identification of stem-like cell subpopulations whose distribution within tumors may be regulated by NME1. Although NME1 itself is not currently a robust marker for malignant progression, its differential expression within tumor subpopulations may aid in the identification of prognostic markers and novel therapeutic targets for melanoma in its advanced stages.

Disclosure of Potential Conflicts of Interest

No potential conflicts of interest were disclosed.

Authors' Contributions

Conception and design: Y. Wang, D.M. Kaetzel
Development of methodology: Y. Wang, M.L. Fisher, R.L. Eckert, D.M. Kaetzel
Acquisition of data (provided animals, acquired and managed patients, provided facilities, etc.): Y. Wang, M.K. Leonard, D.E. Snyder, R.L. Eckert, D.M. Kaetzel
Analysis and interpretation of data (e.g., statistical analysis, biostatistics, computational analysis): Y. Wang, M.K. Leonard, D.E. Snyder, R.L. Eckert, D.M. Kaetzel
Writing, review, and/or revision of the manuscript: Y. Wang, M.K. Leonard, D.M. Kaetzel
Administrative, technical, or material support (i.e., reporting or organizing data, constructing databases): D.M. Kaetzel
Study supervision: D.M. Kaetzel

Acknowledgments

This work was supported by research grants R01 CA83237, R01 CA159871, and R01 CA159871-S1 (D.M. Kaetzel) from the NIH/NCI, research grants R01 CA211909 and R01 CA184027 (R.L. Eckert) from the NIH/NCI, training grant T32 CA154274 (Antalis) from NIH/NCI, research education grant R25 GM055036 (Summers) from the National Institute of General Medical Sciences, and a research grant from the Maryland Stem Cell Research Foundation (MSCRFI-1638, D.M. Kaetzel).

The costs of publication of this article were defrayed in part by the payment of page charges. This article must therefore be hereby marked *advertisement* in accordance with 18 U.S.C. Section 1734 solely to indicate this fact.

Received January 8, 2018; revised June 14, 2018; accepted May 16, 2019; published first May 23, 2019.

References

1. Lee N, Barthel SR, Schatton T. Melanoma stem cells and metastasis: mimicking hematopoietic cell trafficking? Lab Invest 2014;94:13–30.
2. Schatton T, Murphy GF, Frank NY, Yamaura K, Waaga-Gasser AM, Gasser M, et al. Identification of cells initiating human melanomas. Nature 2008; 451:345–9.
3. Boiko AD, Razorenova OV, van de Rijn M, Swetter SM, Johnson DL, Ly DP, et al. Human melanoma-initiating cells express neural crest nerve growth factor receptor CD271. Nature 2010;466:133–7.
4. Civenni G, Walter A, Kobert N, Mihic-Probst D, Zipser M, Belloni B, et al. Human CD271-positive melanoma stem cells associated with metastasis establish tumor heterogeneity and long-term growth. Cancer Res 2011;71: 3098–109.
5. Smith SC, Theodorescu D. Learning therapeutic lessons from metastasis suppressor proteins. Nat Rev Cancer 2009;9:253–64.
6. Steeg PS, Bevilacqua G, Kopper L, Thorgeirsson UP, Talmadge JE, Liotta LA, et al. Evidence for a novel gene associated with low tumor metastatic potential. J Natl Cancer Inst 1988;80:200–4.
7. Marino N, Nakayama J, Collins JW, Steeg PS. Insights into the biology and prevention of tumor metastasis provided by the Nm23 metastasis suppressor gene. Cancer Metastasis Rev 2012;31:593–603.
8. Ouatas T, Salerno M, Palmieri D, Steeg PS. Basic and translational advances in cancer metastasis: Nm23. J Bioenerg Biomembr 2003;35:73–9.
9. Salerno M, Palmieri D, Bouadis A, Halverson D, Steeg PS. Nm23-H1 metastasis suppressor expression level influences the binding properties, stability, and function of the kinase suppressor of Ras1 (KSR1) Erk scaffold in breast carcinoma cells. Mol Cell Biol 2005;25:1379–88.
10. Horak CE, Lee JH, Elkahloun AG, Boissan M, Dumont S, Maga TK, et al. Nm23-H1 suppresses tumor cell motility by down-regulating the lysophosphatidic acid receptor EDG2. Cancer Res 2007;67:7238–46.
11. McCorkle JR, Leonard MK, Kraner SD, Blalock EM, Ma D, Zimmer SG, et al. The metastasis suppressor NME1 regulates expression of genes linked to metastasis and patient outcome in melanoma and breast carcinoma. Cancer Genomics Proteomics 2014;11:175–94.
12. Kaetzel DM, Leonard MK, Cook GS, Novak M, Jarrett SG, Yang X, et al. Dual functions of NME1 in suppression of cell motility and enhancement of genomic stability in melanoma. Naunyn Schmiedebergs Arch Pharmacol 2015;388:199–206.
13. Yang M, Jarrett SG, Craven R, Kaetzel DM. YNK1, the yeast homolog of human metastasis suppressor NM23, is required for repair of UV radiation- and etoposide-induced DNA damage. Mutat Res 2009;660:74–8.

14. Fisher ML, Adhikary G, Grun D, Kaetzel DM, Eckert RL. The Ezh2 polycomb group protein drives an aggressive phenotype in melanoma cancer stem cells and is a target of diet derived sulforaphane. Mol Carcinog 2016;55: 2024–36.
15. Sztiller-Sikorska M, Koprowska K, Jakubowska J, Zalesna I, Stasiak M, Duechler M, et al. Sphere formation and self-renewal capacity of melanoma cells is affected by the microenvironment. Melanoma Res 2012;22:215–24.
16. Yang T, Rycaj K, Liu Z-M, Tang DG. Cancer stem cells: constantly evolving and functionally heterogeneous therapeutic targets. Cancer Res 2014;74: 2922–7.
17. Roesch A, Fukunaga-Kalabis M, Schmidt EC, Zabierowski SE, Brafford PA, Vultur A, et al. A temporarily distinct subpopulation of slow-cycling melanoma cells is required for continuous tumor growth. Cell 2010;141:583–94.
18. Schatton T, Frank MH. The in vitro spheroid melanoma cell culture assay: cues on tumor initiation? J Invest Dermatol 2010;130:1769–71.
19. Boissan M, Lacombe ML. Learning about the functions of NME/NM23: lessons from knockout mice to silencing strategies. Naunyn-Schmiedeberg's Arch Pharmacol 2011;384:421–31.
20. Leone A, Flatow U, VanHoutte K, Steeg PS. Transfection of human nm23-H1 into the human MDA-MB-435 breast carcinoma cell line: effects on tumor metastatic potential, colonization and enzymatic activity. Oncogene 1993;8:2325–33.
21. Zhang Q, McCorkle JR, Novak M, Yang M, Kaetzel DM. Metastasis suppressor function of NM23-H1 requires its 3';-5' exonuclease activity. Int J Cancer 2011;128:40–50.
22. Valent P, Bonnet D, De Maria R, Lapidot T, Copland M, Melo JV, et al. Cancer stem cell definitions and terminology: the devil is in the details. Nat Rev Cancer 2012;12:767–75.
23. Lakso M, Steeg PS, Westphal H. Embryonic expression of nm23 during mouse organogenesis. Cell Growth Differ 1992;3:873–9.
24. Gervasi F, D'Agnano I, Vossio S, Zupi G, Sacchi A, Lombardi D. nm23 influences proliferation and differentiation of PC12 cells in response to nerve growth factor. Cell Growth Differ 1996;7:1689–95.
25. Lim JQ, Lu J, He BP. Diva/BclB regulates differentiation by inhibiting NDPKB/Nm23H2-mediated neuronal differentiation in PC-12 cells. BMC Neurosci 2012;13:123.
26. Novak M, Jarrett SG, McCorkle JR, Mellon I, Kaetzel DM. Multiple mechanisms underlie metastasis suppressor function of NM23-H1 in melanoma. Naunyn Schmiedebergs Arch Pharmacol 2011;384:433–8.
27. Hartsough MT, Steeg PS. Nm23/nucleoside diphosphate kinase in human cancers. J Bioenerg Biomembr 2000;32:301–8.
28. Hu Y, Smyth GK. ELDA: extreme limiting dilution analysis for comparing depleted and enriched populations in stem cell and other assays. J Immunol Methods 2009;347:70–8.